ELSEVIER

Chemical Engineering Journal 135S (2008) S147–S152

Chemical Engineering Journal

www.elsevier.com/locate/cej

Multi-scale modeling of microstructured reactors for the oxidative dehydrogenation of ethane to ethylene

Bin Yang *, Tom Yuschak, Terry Mazanec, Anna Lee Tonkovich, Steve Perry

Velocys, Inc., 7950 Corporate Boulevard, Plain City, OH 43016, USA

Abstract

A novel ethylene production process has been developed via oxidative dehydrogenation of ethane in microstructured reactors. This process, where hydrogen is combusted in close contact with the endothermic dehydrogenation reaction, has the potential to significantly improve the economics of ethylene production. The oxidative dehydrogenation reactor walls are coated with a novel catalyst that enables both high activity and high selectivity to ethylene. Overall reactor performance has exceeded 75% ethane conversion and 84% ethylene selectivity without performance degradation over several 100 h in laboratory experiments. The reactor operated with a peak temperature near 950 °C and a reaction contact time less than 50 ms. Single pass ethylene yield far exceeded that possible in a conventional stream cracker.

Reactor design was enabled by the use of computational flow dynamic (CFD) models at three levels: local, intermediate and global. A local model reduced the set of kinetic equations to a manageable few. An intermediate model assessed the reactor performance in a single channel with a simplified set of kinetics. A global model set the required performance parameters, including flowrate per reactor volume, conversion and selectivity for practical, commercial implementation in a reactor with thousands of parallel microchannels.

Keywords: CFD; Ethane; Ethylene; Heterogeneous reactions; Kinetics; Microstructure reactor; Oxidative dehydrogenation

1. Introduction

The current work integrates both an efficient new form of the hydrogen oxidation catalyst with a reactor design that controls the reaction time, temperature, and composition to improve overall selectivity and conversion. Experimental reactor results using a microchannel reactor show that ethane can be oxidized to ethylene with both selectivity and conversion greater than 80% [1].

High yields of ethylene have been achieved in microchannel ethane ODH reactors, whose designs were supported by multi-scale modeling at three scales. First, local models reduce the complex reaction network, which exceeds 100 elementary steps, to a manageable few. Second, intermediate models used the simplified network in reactor models that include reactor hydrodynamics with detailed local mass and heat balances for a slice of a commercial reactor. Finally, global models are used to aggregate performance of many parallel reactor slices, as predicted by intermediate models, to assess overall performance of a commercial full-scale reactor. This multi-scale modeling methodology gave reasonable predictions for the experimental performance of a thermally integrated microstructured reactor.

The local model includes the complicated reaction network of more than 100 homogeneous reaction elementary steps reported in the literature [2–4]. Detailed kinetics was included in a small volume reactor model and solved using CFD models. The impact of the kinetics parameters on the overall reaction rates has been investigated. Based on these sensitivity studies in the local model, a small subset of homogeneous reactions were chosen whose rates are controlling. Next, a number of candidate heterogeneous reactions that occur simultaneously with the homogeneous reactions were tested for their effect on the model predictions. These reactions were evaluated and compared with experimental data for the novel coated catalyst system and the reactions that gave the best fit were selected for inclusion in the model. The set of controlling gas phase and surface reactions includes a step for the formation of carbon, which is a critical reaction to control in order to maintain operability within the microstructured reactor.

The full suite of homogeneous and heterogeneous kinetics developed in local models was validated using single channel catalyst testing reactors. The reactors were operated in an integral mode, where the mass and heat transfers also affect the performance. Detailed CFD modeling of the single channel

* Corresponding author. Tel.: +1 614 733 3393; fax: +1 614 733 3301.
E-mail address: yangbin@velocys.com (B. Yang).

1385-8947/$ – see front matter © 2007 Elsevier B.V. All rights reserved.
doi:10.1016/j.cej.2007.07.050

test reactor was developed to compare model predictions with experiments.

The validated local models were used in detailed intermediate models to describe a slice or single channel of a full-scale reactor. The intermediate models include preheat of the reactants in an attached microchannel heat exchange channel, the high temperature reaction zone, and a second heat exchange section to quickly quench the product mix. The CFD models include all reactor hydrodynamic effects, heat transfer, mass transfer, and the reduced set of controlling heterogeneous and homogeneous reactions. The predicted performance of the intermediate model was also validated with a test reactor. The intermediate model results were used in a global model to predict the performance of an individual full-scale commercial reactor. This report describes the development of the three levels of computational models.

2. Background

Ethylene is an important commodity chemical. It is used as a feedstock for many chemicals and polymers. Conventional ethylene production is carried out through energy intensive hydrocarbon steam cracking, which involves heating hydrocarbon feedstocks and steam to extremely high temperatures at nearly atmospheric pressures in furnaces. This process is both energy and capital intensive. An alternative process for ethylene production is the oxidative dehydrogenation (ODH) of ethane, reviewed recently by Schmidt and others [5]. This process has been under development for more than two decades in various laboratories around the world. The hurdles encountered by these ODH development programs are numerous, but commonly involve the limitation of conventional processing equipment.

In the development of ethane ODH, obtaining high selectivity to ethylene is a key challenge. Using platinum (Pt) as the catalyst on a ceramic foam monolith support Huff and Schmidt [6] achieved 65% ethylene selectivity and 70% ethane conversion at a 5 ms contact time and 1000 °C. Major by-products CO and CO_2 account for 25% of the converted ethane. A significant improvement in ethylene selectivity is reported when hydrogen is added to the process stream with the molar ratio of hydrogen to oxygen at two to one [7].

In more recent work, Henning and Schmidt [8] reported 83% ethylene selectivity and 75% conversion with hydrogen added to the process stream. These results are based on a Pt–Sn catalyst which consistently showed better performance than a pure Pt. Henning's test reactor was a 19 mm ID quartz tube. The catalyst was coated on alumina foam monolith of 10 mm long placed in the quartz tube, followed by a 20 cm long homogeneous reaction zone. Comparative experiments with and without hydrogen addition showed that the overall ethylene selectivity is improved significantly, from 67% to 83% when hydrogen is added, at the same ethane conversion of 64%. Ethylene selectivity is improved with hydrogen addition because the dominating chemistry on the catalyst surface is hydrogen combustion which occurs faster than hydrocarbon surface oxidation. The heat from the catalyzed hydrogen combustion drives the homogeneous endothermic dehydrogenation of ethane to ethylene.

The current work integrates both an efficient new form of the hydrogen oxidation catalyst with a reactor design that controls the reaction time, temperature, and composition to improve overall selectivity and conversion. Experimental reactor results using a microchannel reactor show that ethane can be oxidized to ethylene with high selectivity at high conversion

3. Experimental

Two microreactors were built from Inconel 617 and operated: (1) a short single channel test device for obtaining kinetic rate data, and (2) a thermally integrated test device for validating model predictions.

3.1. Short single channel kinetics reactor

The short single channel, shown in Fig. 1 (not to scale), was made from a 12.7 mm diameter Inconel 617 rod. A through channel was cut along the center axis of the rod with a rectangular cross sectional shape. Two straight parallel channels are formed after the insertion of the coupon train, each with a constant cross section of 0.51 mm by 7.37 mm. The coupon train consisted of three coupons of the same cross section 3.2 mm by 8.5 mm inserted from one end in series, with only the centermost coupon in the train having the catalyst applied thereon for experiments involving catalyst. The coupons were tightly fitted inside the housing and it was expected their locations were fixed during the test. A Pt–Sn catalyst (2.4:1 atomic) was directly coated on the coupon surface [9]. For experiments with a catalyst, the active metals were coated on the coupon surfaces only, not on the reactor housing inner surfaces. Gas mixtures of ethane, hydrogen, and oxygen were prepared by metering each gas individually via Brooks mass flow controllers and mixing in a tee ~45 cm upstream of the test device. Temperature measurements in the cylindrical test device were made via three thermocouples: (1) upstream of the catalyst coupon, (2) downstream portion of the catalyst coupon, and (3) outer wall of the reactor.

Blank tests were performed in the short channel test device without catalyst. These experiments included ethane cracking tests where only ethane and steam were fed and tests with oxygen added. Results from these tests were used to establish the cracking and oxidation rates in the absence of catalyzed heterogeneous reactions. A catalyst coated coupon was then introduced and the tests were repeated. Kinetic rate data were gathered over a wide range of oxidation conditions as shown in Table 1, varying temperature, flow rate, and inlet composition. For a few of the tests air was fed to supply O_2. For most tests using the short single channel test device, O_2 gas was fed with a trace of nitrogen (5% of the total volumetric flow). The carbon balance generally was always within ±20%, and typically within ±5%, both on a

Table 1
Range of experimental inlet conditions used for kinetic rate data

Inlet reactor temperature (°C)	800–1000
C_2H_6:H_2:O_2 ratio	2:2:1 to 10:2:1
Total flow rate (SLPM)	0.84–3.42

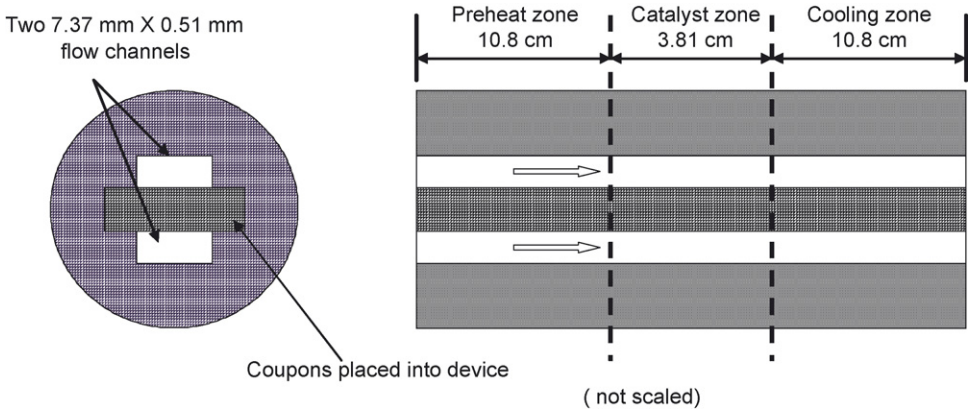

Fig. 1. Cylindrical test device used to collect kinetic rate data for local models.

measured and calculated dry flow rate basis, and only the data within the latter carbon balance range was included in the data analysis. It was believed that the few high carbon balance cases were due to the errors in GC calibration at the beginning of the test and it was corrected later.

3.2. Thermally integrated reactor

The thermally integrated test device (Fig. 2) included counter-current heat exchange with the adjacent product cooling channel. Heat produced in the hydrogen combustion reaction is transferred to the cracking reaction. Pure oxygen was fed into a separate channel in the device and injected into the reaction channel (containing the pre-mixed ethane, hydrogen and nitrogen tracer gases) through a narrow slot upstream of the catalytic hydrogen combustion zone. This allows time for the reactants to fully mix upstream of the hydrogen combustion catalyst. The device was operated with the hot zone inside a clamshell resistance heater to offset heat losses and help with start-up. The thermally integrated reactor was operated with a Pt-alloy catalyst applied *ex situ*, by the same method described previously, to two 11.4 cm by 2.3 cm coupons that are laid side by side in the device to form two parallel channels.

In most experiments, the total inlet flow was maintained at 10 SLPM (standard liters per minute at 0 °C and 1 atm), a typical run used 3.46 SLPM C_2H_6, 5.18 SLPM H_2, and 0.5 SLPM N_2, fed to the reactant inlet and 0.86 SLPM O_2 fed to the oxygen inlet. External body temperatures were measured along the length of the reactor using type K thermocouples. During operation, the test device was operated with a maximum temperature of ~965–970 °C, and an outlet pressure of 103 kPa. Typically, the inlet streams were fed at 200 °C or less and the product stream exited the device at about 400 °C. The carbon balance during operation of the thermally integrated test device was typically within ±5%.

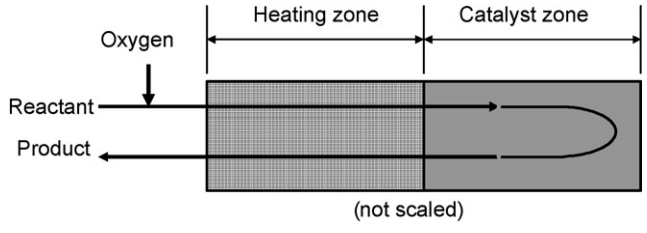

Fig. 2. Thermally integrated test device used to collect ethane cracking model validation data.

For both test devices, inlet gas flows were metered via Brooks mass flow controllers and dry outlet gas concentrations were measured by an Agilent gas chromatograph (GC), which was calibrated daily. Dry outlet flow rate was measured by a dry test meter. The GC based ethane conversion and selectivity to any species i, which may be expressed as a fraction or a percent, were calculated as

$$\%\ \text{Ethane conversion} = 100 \times \left(\frac{1 - C\ \text{in ethane in product stream}}{C\ \text{in ethane fed}} \right) \quad (1)$$

$$\%\ \text{Ethylene selectivity} = 100 \times \frac{C\ \text{in ethylene product}}{\Sigma\, C\ \text{in all products}} \quad (2)$$

Additionally, the ethane conversion was calculated based on the nitrogen tracer flow as follows

$$\chi_{C_2H_6} = 1 - \frac{F_{N_2,\text{in}}}{F_{C_2H_6,\text{in}}} \left(\frac{y_{C_2H_6}}{y_{N_2}} \right)_{\text{dry outlet gas}} \quad (3)$$

Where y_i is the mole fraction of species i in the dry outlet gas stream and $F_{i,\text{in}}$ is the mole flow rate of species i at the inlet. Agreement between the conversion as calculated via the GC and nitrogen tracer methods was typically within 5%.

4. CFD model development

4.1. Reactor modeling strategy

The reactive flow models were developed at three scales to assist the reactor design. A local model was developed to reduce the complex reaction network from over a 100 elementary steps to a manageable few. Reaction steps were chosen for the next level of modeling on the basis of their impact on the heat balance and product distribution. An intermediate model was developed using the reduced network in a reactor model with precise geometrical rendering that includes reactor hydrodynamics with

detailed local mass and heat balances for a slice or single channel of a commercial reactor. A global model was then developed to calculate the aggregate performance of many parallel reactor slices to assess overall performance of a commercial full-scale reactor.

Several detailed gas phase ethane oxidation mechanisms can be found in the literature. Under fuel rich conditions, the mechanism proposed by Marinov and others [2] contains 722 reversible reactions involving 161 species. In the Mims-Dean mechanism [3] there are 450 reversible reactions and 115 species. The complexity of these detailed chemistries limits the wide spread application of these mechanisms in chemical reactor design. There are efforts to bridge the academic approaches and the common practice of engineering by reducing the size of the reaction network. Zerkle and others [4] reduced the ethane oxidation mechanism to a subset containing only H, C1 and C2 chemistry. Still 131 reversible reactions and 25 species comprise the reduced mechanism.

In this work, the full set of gas phase reactions involved in ethane oxidation dehydrogenation chemistry is reduced to a small set suitable for extensive reactor modeling and design. Reactions were chosen to provide the most impact on the thermal balance of the system and explain the most important products. When deriving this simplified set of reactions, the following criteria are applied to exclude the least critical reactions for the type of reactor and operating conditions of interest in this work.

- Reactions important only at high temperature (>1100 °C) were excluded based on the lower temperature operation of this process (less than 1000 °C).
- Reactions leading to high concentrations of products not experimentally observed were excluded.
- Reactions focusing on H and C1–C4 carbon species were included, as is one coke forming reaction that is meant to provide a simple representation of the entire reaction sequence leading to coke formation.

For heterogeneous chemistry, the potentially important reactions were postulated from literature studies of others in similar systems. However, even with the same catalytically active ingredients, the catalyst performance may vary significantly depending on the way the catalyst is formulated and other factors. Oxidation reactions of methane, ethane, ethylene, acetylene and hydrogen were considered. The heterogeneous kinetics proposed in this work was validated based on the experimental catalyst performance data. The reactions that were found to be sufficient to describe are shown in Table 2.

4.2. Governing equations

The energy equation solved has standard form

$$\frac{\partial}{\partial t}(\rho E) + \nabla(\vec{v}(\rho E + p)) = \nabla\left(k\nabla T - \sum_j h_j \vec{J}_j\right) + S_\mathrm{h} \quad (4)$$

where, k is thermal conductivity of gas mixture, ρ is density of the gas mixture, J_j is diffusion flux of species j, v is velocity, T is temperature, p is pressure and S_h is the source term—the heat of chemical reactions.

In equation (4),

$$E = h - \frac{p}{\rho} + \frac{v^2}{2} \quad (5)$$

where sensible enthalpy h is defined for ideal gas as

$$h = \sum_j Y_j h_j \quad (6)$$

where Y_j is the mass fraction of species j and

$$h_j = \int_{T_\mathrm{ref}}^{T} c_{p,j}\,\mathrm{d}T \quad (7)$$

where $C_{p,j}$ is heat capacity of species j and T_ref is 298.15 K.

The heat source term is solely due to chemical reactions which is calculated as

$$S_\mathrm{h} = -\sum \frac{h_j^0}{M_j} R_j \quad (8)$$

where h_j is the enthalpy of formation of species of j, M_j is molecular weight and R_j is the volumetric rate of creation of species j.

The mass conservation equation of species j takes the following general form:

$$\frac{\partial}{\partial t}(\rho Y_j) + \nabla(\rho\vec{v}Y_j) = -\nabla\vec{J}_j + R_j \quad (9)$$

An equation of this form will be solved for $N-1$ species where N is the total number of species in the mixture.

The diffusion flux of species j, is calculated by

$$\vec{J}_j = -\rho D_{j,m}\nabla Y_j \quad (10)$$

Here $D_{j,m}$ is the diffusion coefficient of species j in the mixture.

The net source of species i due to chemical reactions is computed as the sum of the Arrhenius reaction sources over the N_R reactions that the species participate in:

$$R_\mathrm{i} = M_\mathrm{i}\sum_{i=1}^{N_\mathrm{R}} \widehat{R}_\mathrm{i,r} \quad (11)$$

where $R_{i,r}$ is the Arrhenius molar rate of creation/destruction of species i in reaction r. In general, for an irreversible reaction, $R_{i,r}$ is given by

$$\widehat{R}_{i,r} = (v''_{i,r} - v'_{i,r})\left(k_r \prod_{j=1}^{N} [C_j]^{(\eta'_{j,r}+\eta''_{j,r})}\right) \quad (12)$$

where C_j is molar concentration of species j, $v'_{i,r}$ is stoichiometric coefficient for reactant i in reaction r, $v''_{i,r}$ is stoichiometric coefficient for product i in reaction r, $\eta'_{j,r}$ is rate exponent for reactant species j in reaction r, $\eta''_{j,r}$ is rate exponent for product j in reaction r and k_r is the rate constant for reaction r.

The rate constant for reaction r, k_r, is computed using the Arrienius expression

$$k_r = A_r\,\mathrm{e}^{-E_r/RT} \quad (13)$$

Table 2
Kinetics of the reactions in ethane oxidative dehydrogenation process concentration C_i are in kmol/m^3

No	Reaction	Rate expressions r in kgmol/m^3 s	A_i	E_i J/kgmol
1	$C_2H_6 \Leftrightarrow C_2H_4 + H_2$	$r_1 = A_1 \exp(-E_1/RT)C_{C_2H_6}$	8.5E8	1.6E8
2	$H_2 + (1/2)O_2 \rightarrow H_2O$	$r_2 = A_2 \exp(-E_2/RT)C_{H_2}C_{O_2}^{0.5}$	3.0E10	1.64E8
3	$C_2H_4 + O_2 \rightarrow 2CO + 2H_2$	$r_3 = A_3 \exp(-E_3/RT)C_{C_2H_4}C_{O_2}$	8.0E12	1.8E8
4	$C_2H_6 + H_2 \rightarrow 2CH_4$	$r_4 = A_4 \exp(-E_4/RT)C_{C_2H_6}$	6.0E9	2.1E8
5	$C_2H_4 \rightarrow C_2H_2 + H_2$	$r_5 = A_5 \exp(-E_5/RT)C_{C_2H_4}$	2.26E11	2.5E8
6	$2C_2H_4 \rightarrow C_4H_8$	$r_6 = A_6 \exp(-E_6/RT)C_{C_2H_4}$	3.5E10	2.4E8
7	$C_2H_2 + C_2H_4 \rightarrow C_3H_6 + C$	$r_7 = A_7 \exp(-E_7/RT)C_{C_2H_4}C_{C_2H_2}$	2.5E16	2.7E8
8	$H_2 + (1/2)O_2 \rightarrow H_2O$ (catalyzed)	$r_8 = A_8 \exp(-E_8/RT)C_{H_2}C_{O_2}^{0.5}$	2100	4.0E7

The pre-exponential factors A_i have the units to give the reaction rates in kgmol/m^3 s, except for reaction 8 which are in units of m^2 *vs.* m^3 to represent a surface reaction.

where A_r is pre-exponential factor, E_r is activation energy for reaction r (J/kmol), R is universal gas constant (J/kmol K).

Finally, the full set of governing equations is completed with the following momentum conservation equation

$$\frac{\partial}{\partial t}(\rho\vec{v}) + \nabla(\rho\vec{v}\vec{v}) = -\nabla p\nabla(\bar{\bar{\tau}}) + \rho\vec{g} \quad (14)$$

The stress tensor is given by

$$\bar{\bar{\tau}} = \mu[(\nabla\vec{v}) + (\nabla\vec{v}^T) - \frac{2}{3}\nabla\vec{v}I] \quad (15)$$

where μ is the molecular viscosity, I is the unit tensor.

5. Results and discussion

5.1. Short single channel kinetics reactor

The set of reactions summarized above were used to fit kinetic parameters for the homogeneous reactions and the catalytic heterogeneous hydrogen combustion reaction. The comparison of experimental versus predicted conversion and selectivity gave reasonable agreement using the set of 8 scoping reactions included in the study as shown in Figs. 3–5. It should be pointed that the test condition for each data point in term of ethane/hydrogen/oxygen ratio, temperature and contact time was different and covered a wide range of interest. In a relative term, the ethane conversion between experiment and model predictions is in a better agreement compared to the ethylene selectivity. And for ethylene selectivity, the agreement between experiment and model predictions are better when it is above 80%, and for most of the conditions, the model over-predicts the ethylene selectivity. Since ethylene selectivity higher than 80% is of interest for this application, the authors concluded

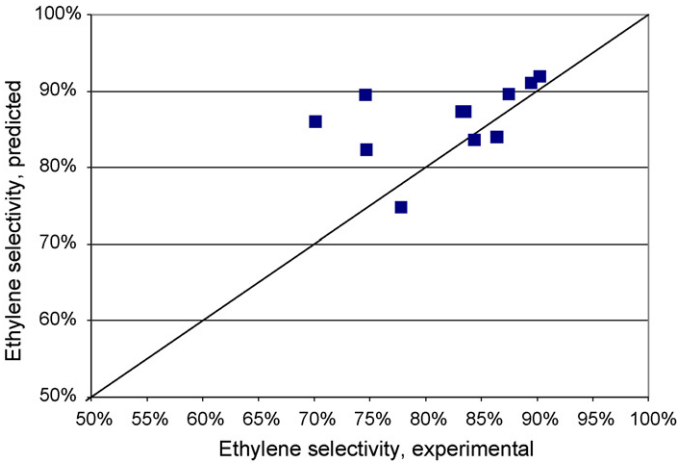

Fig. 4. Reconciliation plot of experimental ethylene selectivity *vs.* predictions.

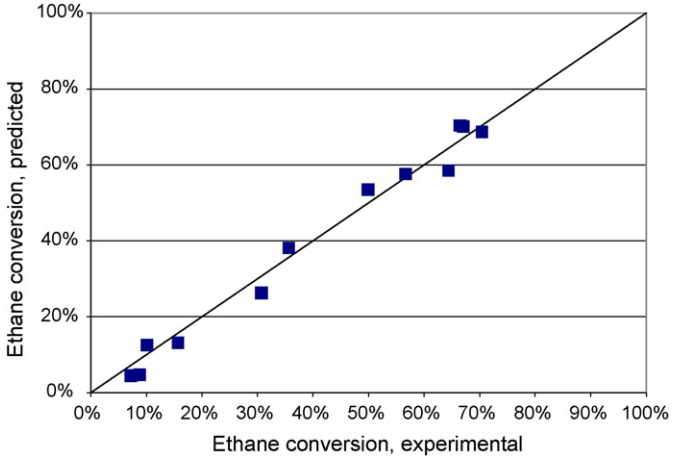

Fig. 3. Reconciliation plot of experimental ethane conversion *vs.* predictions.

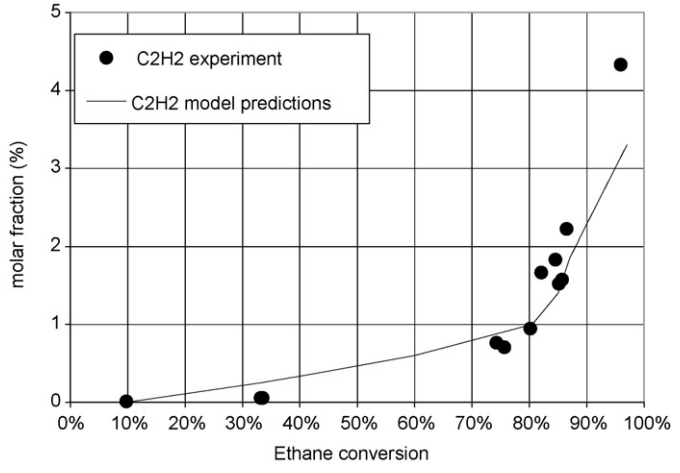

Fig. 5. Comparison of model predictions with experimental data for acetylene production in the short single channel reactor. Feed composition: C_2H_6:H_2:O_2 = 3:2:1, temperature: 700–850 °C.

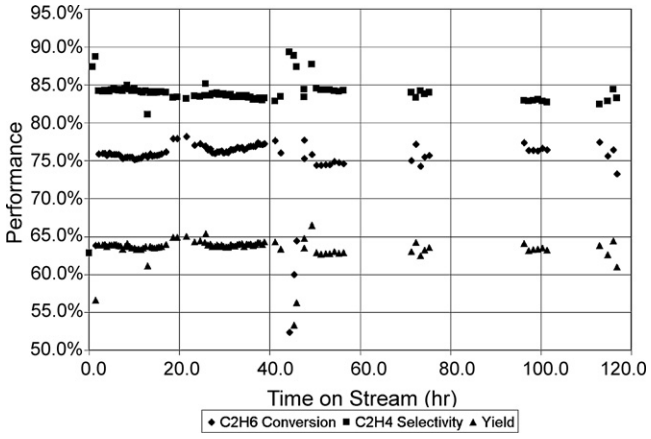

Fig. 6. Results of thermally integrated test device showing performance *vs*. TOS in hours at 3.3:4:1 ethane:hydrogen:oxygen ratio.

Table 3
CFD model predictions for thermally integrated reactor

Composition	Ethane conversion (%)	Ethylene selectivity (%)	Oxygen conversion (%)
Model predictions			
2:2:1	82	90	100
4:2:1	78	90	100
3:2:1	82.5	90	100

that for the purpose of engineering design of the reactor, the kinetics model is adequate.

In Fig. 5, the acetylene molar fraction in the product is plotted versus ethane conversion for both the test data and the model predictions. Between 80–85% ethane conversions, the experiment data showed a steep increase of acetylene concentration in the effluent of the reactor. The model essentially (unsmoothed solid line) is able to capture this increase at ~80% ethane conversion. The sharp slope change of the model prediction curve is a result of insufficient number of model results.

5.2. Thermally integrated reactor

The thermally integrated reactor operated with steady operation for more than 100 h. The formation of ethylene from ethane is a notorious coke producing reaction, which is always a concern for microchannel operation. At a flowrate of 10 SLPM and a C_2H_6:H_2:O_2 ratio of 3.3:4:1, a steady ethane conversion greater than 75% was obtained with a selectivity to ethylene greater than 83% as shown in Fig. 6. Fig. 6 shows the TOS plot for pressure drop and temperature, where steady performance is noted. There was a heater upset around 40–50 h which is also reflected in Fig. 6. Little carbon build up was observed in the device after operation.

The model results for the thermally integrated reactor predict slightly higher conversion and selectivity than the experimentally observed conversion of 75% and selectivity of 83%, but overall the agreement was reasonable for a complex reaction and design in view of the simplified set of reactions used (Table 3).

6. Conclusions

Multi-level modeling has proven useful for the design and computational simulation of microchannel reactors for ethane ODH to produce ethylene. Simplification of the kinetic network in a local model permits more complex models to be tested within manageable computation times. Simulation predictions are within reasonable agreement of the experimental results. Ethane ODH in a microchannel device has been shown to provide high conversion of ethane and selectivity of ethylene.

Acknowledgements

The authors acknowledge contributions from DOW Chemicals and the US Department of Energy for financial support.

References

[1] T.J. Mazanec, Olefins by high intensity oxidation of ethane, in: AIChE Meeting, Atlanta, April, 2005.
[2] N.M. Marinov, W.J. Pitz, W.J. Westbrook, M.J. Castaldi, S.M. Senkan, Modeling of aromatic and polycyclic aromatic hydrocarbon formation in premixed methane and ethane flames, Combust. Sci. Technol. 116–117 (1996) 211–287.
[3] C.A. Mims, R. Mauti, A.M. Dean, K.D. Rose, Radical chemistry in methane oxidative coupling: tracing of ethylene secondary reactions with computer models and isotopes, J. Phys. Chem. 98 (1994) 13357–13372.
[4] D.K. Zerkle, M.D. Allendorf, M. Wolf, O. Deutschmann, Understanding homogeneous and heterogeneous contributions to the platinum-catalyzed partial oxidation of ethane in a short-contact-time reactor, J. Catal. 196 (2000) 18–39.
[5] L.D. Schmidt, J. Siddall, M. Bearden, New ways to make old chemicals, AICHE J. 46 (2001) 1492–1495.
[6] M. Huff, L.D. Schmidt, Olefin and syngas formation by direct catalytic oxidation of ethane at short contact time, J. Phys. Chem. 97 (1993) 11815–11822.
[7] A. Bodke, D. Olschki, L.D. Schmidt, E. Ranzi, High selectivities to ethylene by partial oxidation of ethane, Science 285 (1999) 712–715.
[8] D.A. Henning, L.D. Schmidt, Oxidative dehydrogenation of ethane at short contact times: species and temperature profiles within and after the catalyst, Chem. Eng. Sci. 57 (2002) 2615–2625.
[9] J.M. Watson, F.P. Daly, T.J. Mazanec, B.Yang, Catalysts having catalytic material applied directly to thermally grown alumina and catalytic methods using same, improved methods of oxidative dehydrogenation, US 2005/0272965, published December 8, 2005.